

CRISM Observations of Persistent Water Ice Deposits in the Northern Plains of Mars. K. D. Seelos¹, F. P. Seelos¹, T. N. Titus², S. L. Murchie¹, and the CRISM Team, ¹JHU Applied Physics Laboratory, 11100 Johns Hopkins Rd., Laurel, MD 20723 (kim.seelos@jhuapl.edu), ²USGS, 2255 N. Gemini Dr., Flagstaff, AZ 86001.

Introduction: Discreet water ice deposits have been observed to persist long into the summer season at fairly low latitudes in the northern plains. Mars Reconnaissance Orbiter (MRO) Compact Reconnaissance Imaging Spectrometer for Mars (CRISM) multispectral data acquired in the northern summer of MY 28 was used to identify and map the furthest south occurrence of these deposits. The deposits are typically associated with north-facing slopes of craters and other topographically elevated terrains. However, comparison to global datasets such as topography, albedo, and Gamma Ray Spectrometer (GRS) dry layer thickness (DLT) yield insight into possible relationships to broader controlling factors. Targeted hyperspectral CRISM observations provide detail of select deposits, and also show smaller deposits that are likely very common throughout the northern plains. It is possible that the Phoenix mission set to land in late May 2008 ($L_s \sim 75^\circ$), at will be able to directly observe one or more of the smaller outliers.

Data Characteristics and Evaluation: CRISM's multispectral survey campaign early in the MRO primary science phase (PSP) achieved nearly complete coverage of the north polar region ($> 65^\circ\text{N}$) in the late summer season ($L_s = 130\text{-}180^\circ$), with 75% coverage at 75°N [1]. The multispectral (MSP) data consist of 72 channels distributed selectively from 0.41 to 3.92 μm [2], and are calibrated to I/F then atmospherically and photometrically corrected prior to mosaicking at 256 pix/deg (~ 230 m/pixel). The spatial resolution and coverage of the MSP dataset allowed for consistent detection of water ice deposits at the ~ 500 meter-scale and larger.

To determine the southernmost extent of the deposits, false-color visible and infrared composites of the MSP dataset as well as a $1.5\mu\text{m}$ band depth map were assembled. 1-degree longitude bins were systematically evaluated and the furthest south occurrence (minimum latitude) of water ice was recorded. For comparison to other datasets, a 10-degree average was calculated. A 10-degree latitude and longitude average value of topography, albedo (as approximated at $1.3\mu\text{m}$), and GRS dry layer thickness was similarly determined about a center latitude of 75°N .

Hyperspectral targeted observations were acquired throughout the northern plains as a result of Phoenix landing site support. Half-resolution (HRL/HRS; 40 m/pixel) and full-resolution (FRT; 20 m/pixel) hyper-

spectral observations have 544 channels from 0.36 to $3.920\mu\text{m}$ [2]. These data are also calibrated to I/F and atmospherically and photometrically corrected following the method demonstrated in [3]. Although the distribution of hyperspectral observations is sparser for this season, the higher spatial resolution allows for detection of an order of magnitude smaller ice deposits (50 to 100 meters, depending on observing mode).

Results: Figure 1 portrays the mapped minimum latitude of water ice occurrence. For large portions of the mosaic, the minimum latitude follows the outline of the residual polar cap. However, km-scale ice outliers frequently exist well away from the cap to as far south as 67°N . The average latitude is 75.5°N . The longitudinal distribution is also not uniform, with a noticeable increase in minimum latitude around lower albedo regions such as Acidalia Planitia ($\sim 300\text{-}345^\circ\text{E}$). Comparison to the GRS DLT [4] also shows remarkable correlation to the inferred ice table depth (Figure 2). This suggests that large-scale factors such as surface albedo are common controls to both surface and subsurface ice distribution.

A majority of the outlying deposits are located on north-facing crater rims or escarpments, but a few appear to extend around to the east and southeast-facing side of the crater rim (Figure 3). The prevalence of ice occurrence in association with craters indicates that

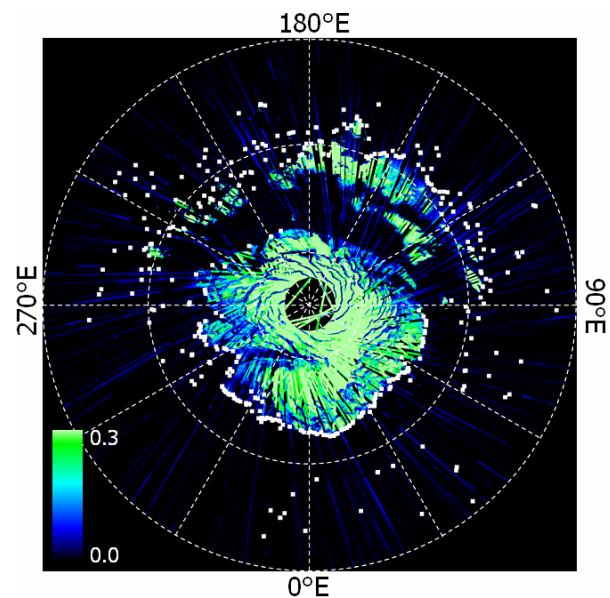


Figure 1. CRISM $1.5\mu\text{m}$ band depth map from $65\text{-}90^\circ\text{N}$ with minimum ice latitudes (white dots).

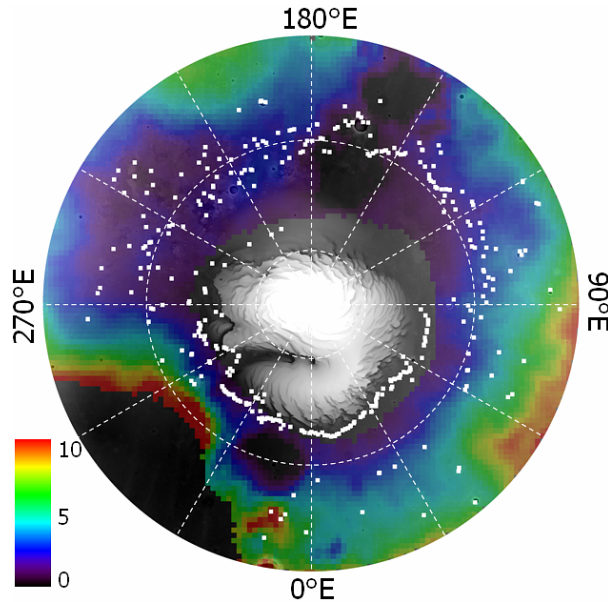


Figure 2. GRS DLT (g/cm^2) over MOLA topography with mapped minimum ice latitude (white dots). Areas with very high and very low DLT values (Acidalia and the polar cap, respectively) have been masked out. Data courtesy of [4].

local slope is a dominant factor controlling the presence of late summer water ice. The deposits that persist on east to southeast-facing sides of craters where readily exposed to morning sunlight are less intuitive. These leeward deposits may be due to orographic lifting that causes wintertime deposition of bright fine-grained CO_2 frost [5]. The CO_2 frost sublimates more slowly than the surrounding CO_2 ice and induces a late spring cold trap that favors accumulation of water ice. Figure 3 shows a hyperspectral observation of one such deposit; the ripple-like morphology of the deposit is further suggestive of aeolian influence. Temperature data from TES and THEMIS observations are also being evaluated to learn more about this process [5].

Conclusion: Outlying late summer water ice deposits are an indication of the extent of environments favorable to interannual persistence of near-surface ice. Spatial distribution, comparison to other datasets, and microenvironment characterization provide insight into the interaction between subsurface, surface, and atmospheric water at high latitudes. During the upcoming spring and northern summer season, CRISM will target these sites with hyperspectral, high spatial resolution observations to monitor the evolution of the water ice deposits through time. CRISM orbital data together with Phoenix ground measurements will also provide an unprecedented coordinated set of surface and atmospheric observations of the martian polar environment.

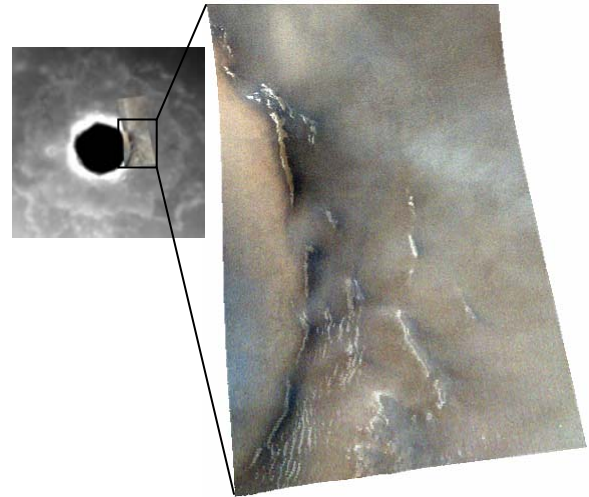


Figure 3. CRISM hyperspectral observation of a southeast-facing water ice deposit (appears white; clouds are also apparent). HRL000044AD was acquired at $L_s=180^\circ$; image is approximately 11 km across at narrowest. False color composite with $R = 0.71\mu\text{m}$, $G = 0.60\mu\text{m}$, $B = 0.53\mu\text{m}$.

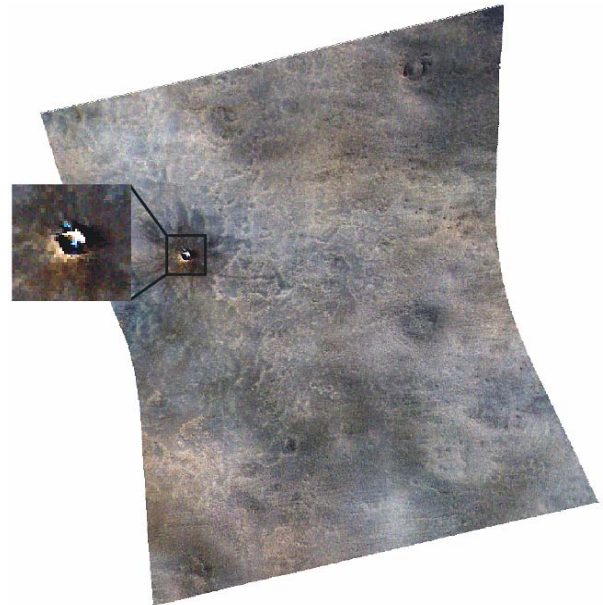


Figure 4. CRISM hyperspectral observation of a small fresh crater with water ice deposit (bluish spots, subset). FRT0000332C was acquired at $L_s = 142.6^\circ$; image is approximately 11 km across at narrowest. False color composite with $R = 0.71\mu\text{m}$, $G = 0.60\mu\text{m}$, $B = 0.53\mu\text{m}$.

References: Seelos et al., (2007) *LPS XXXVIII*, Abstract # 2336. [2] Murchie et al., (2006), *JGR*, 112, E05S03 [3] Murchie et al (2007), *Nature*, in press. [4] Boynton et al. (2006) *LPS XXXVII*, Abstract # 2376. [5] Beitia et al., (2008) *this conference*.